Retinal Thickness and Subnormal Retinal Oxygenation Response in Experimental Diabetic Retinopathy

Hongmei Luan,[1] *Robin Roberts,*[1] *Matthew Sniegowski,*[1] *Dennis J. Goebel,*[1] *and Bruce A. Berkowitz*[1,2]

Purpose. To test the hypothesis that subnormal retinal oxygenation response (ΔPo_2) found at 3 months of experimental diabetes is associated with cellular swelling and increased retinal thickness.

Methods. Two groups of animals were studied: control rats injected intraperitoneally with either 15% body weight of saline or distilled water (cellular swelling model) or with intravitreal *N*-methyl-D-aspartate (NMDA) and 3-month-old diabetic and age-matched control rats. Intraocular pressure and retinal thickness was assessed using an applanation tonometer or high-resolution MRI (23.4 μm^2 in-plane). In separate studies, functional MRI was used to measure blood-retinal barrier (BRB) integrity after Gd-DTPA injection intravenously and retinal ΔPo_2 during carbogen provocation.

Results. Inner and total retinal thickness were lower ($P < 0.05$) after NMDA injection, not different ($P > 0.05$) between control, before and after saline injection and before distilled water injection, and supernormal ($P < 0.05$) after distilled water injection. In diabetic rats, thickness was normal ($P > 0.05$) at most distances from the optic nerve but was subnormal ($P < 0.05$) in superior retina (0.5 mm from the optic nerve). Intraocular pressure was not different ($P > 0.05$) between groups. BRB was intact ($P > 0.05$) after saline and distilled water injection. ΔPo_2 was normal ($P > 0.05$) after saline injection and over inferior hemiretina of the diabetic group but was subnormal ($P < 0.05$) after distilled water injection and over superior hemiretina of diabetic rats.

Conclusions. The lack of increased thickness in 3-month-old diabetic rats in vivo raises the possibility that intracellular swelling is unlikely to underlie subnormal ΔPo_2 in experimental diabetes. In diabetic rats, the spatial disconnect between subnormal ΔPo_2 pansuperiorly and retinal thinning only superiorly to the optic nerve suggests that neurovascular coupling is perturbed. (*Invest Ophthalmol Vis Sci.* 2006;47:320–328) DOI:10.1167/iovs.05-0272

The retinal oxygenation response to a hyperoxic provocation (ΔPo_2), measured by functional MRI, is a powerful and noninvasive biomarker of the ability of the retinovascular system to oxygenate.[1–3] We have shown in rats that during a carbogen (a gas mixture of carbon dioxide [5% CO_2] or an oxygen [95% O_2]) inhalation challenge, retinal ΔPo_2 is elevated relative to 100% oxygen breathing and that retinal ΔPo_2 is significantly lower than normal after 3 months of experimental diabetes.[2,4–7] Furthermore, retinal ΔPo_2 measurements at 3 months correctly predicted histopathologic outcome to treatments for diabetic retinopathy, such as aminoguanidine.[6] Importantly, we have also shown that ΔPo_2 measurement can be adapted to clinical testing (Trick G, et al. *IOVS* 2005;46:ARVO E-Abstract 1413).[1]

The impact of an abnormality associated with diabetes, such as retinal edema, on retinal ΔPo_2 has not yet been examined. Retinal edema is not usually measured directly but is inferred from increased retinal thickness (measured, for example, by optical coherence tomography) and may be caused by fluid accumulation in intracellular or extracellular compartments. Clinically, retinal edema is commonly associated with visual impairment.[8] Studies of cerebral edema demonstrate that intracellular swelling produces microcirculatory compression and impaired hemodynamics.[9] A hallmark of intracellular edema/cellular swelling is that it develops through an osmotic imbalance between blood and tissue and without opening of the blood tissue barrier. We found no evidence for passive blood-retinal barrier (BRB) leakage in vivo until after 6 months of diabetes, suggesting that if retinal edema does occur in diabetic rats, it may be caused by intracellular, and not extracellular, fluid accumulation.

We hypothesized that subnormal ΔPo_2 found in 3-month experimental diabetic retinopathy is linked to cellular swelling and increased retinal thickness. This study had two goals: to determine the impact of intracellular fluid accumulation on retinal ΔPo_2 in a nondiabetic model of cellular swelling and to determine whether thickness is increased at 3 months after the induction of diabetes in rats.

Methods

Animals were treated in accordance with the NIH Guide for the Care and Use of Laboratory Animals and the ARVO Statement for the Use of Animals in Ophthalmic and Vision Research.

Animal Models

NMDA Injection. Control Sprague–Dawley rats were anesthetized with isoflurane and given 6 μL intravitreal injection containing 200 nmol NMDA (Sigma, St Louis, MO) neutralized in 0.01 M phosphate-buffered saline (PBS). All injections were administered in the nasal-temporal quadrant at the ora serrata using a modified 35-gauge needle and aided with a dissection scope. Intravitreal injections were administered over a 1-minute period, and eyes were allowed to acclimate for 1 additional minute before the needle was removed. At 7 or 30 days, MRI experiments were performed to assess retinal thickness changes. Retinal thickness measurements were not different between 7 and 30 days, and the data presented were combined.

Osmotic Provocation. Urethane-anesthetized (1.5 g/kg, 0.083 mL of a 36% solution of urethane/20 g animal weight, intraperitoneally, freshly made daily; Aldrich, Milwaukee, WI) control Sprague–Dawley

From the [1]Department of Anatomy and Cell Biology and the [2]Kresge Eye Institute, Wayne State University, Detroit, Michigan.

Supported by National Institutes of Health Grants EY013831 (BAB) and EY014430 (DJG) and by the Juvenile Diabetes Research Foundation (BAB).

Submitted for publication March 3, 2005; revised June 28 and August 17, 2005; accepted November 3, 2005.

Disclosure: **H. Luan**, None; **R. Roberts**, None; **M. Sniegowski**, None; **D.J. Goebel**, None; **B.A. Berkowitz**, None

The publication costs of this article were defrayed in part by page charge payment. This article must therefore be marked "*advertisement*" in accordance with 18 U.S.C. §1734 solely to indicate this fact.

Corresponding author: Bruce A. Berkowitz, Department of Anatomy and Cell Biology, Wayne State University School of Medicine, 540 E. Canfield, Detroit, MI 48201; baberko@med.wayne.edu.

rats were injected intraperitoneally with 15% of their body weight of either warmed saline or distilled water in three 5% increments administered in sequential 5-minute intervals. This injection schedule was developed to minimize rat deaths inside the magnet that tended to occur if a single bolus was administered (preliminary data not shown). High-resolution magnetic resonance images were obtained before and 2 hours after intraperitoneal injections, followed by the collection of functional MRI data for analysis of retinal ΔPo_2 and BRB integrity. The 2-hour time point was chosen because this is when, after 15% distilled water administered intraperitoneal, gray matter edema develops.[10] One rat in the distilled water group was removed from the final analysis because it had too much motion artifact. In separate benchtop experiments, intraocular pressure (IOP) was assessed directly using an applanation tonometer (Tono-Pen XL; Medtronic, Minneapolis, MN).[11] In urethane-anesthetized control rats, with core temperatures maintained between 35.5°C and 37°C, IOP measurements (average, 25) were obtained before or after, or both, 15% distilled water injection using the same injection schedule described. In addition, IOP was indirectly estimated from the globe circumference measured on MRI.

Diabetic Rats. Separate groups of control (C) Sprague–Dawley rats, and 3-month-old diabetic (D) Sprague–Dawley rats were studied. In rats, diabetes was induced with intraperitoneal injection of streptozocin (55 mg/kg) within 5 minutes of its preparation in 0.01 M citrate buffer, pH 4.5, in rats with body weights of approximately 200 g after overnight fast. Diabetes was verified 3 days later by the presence of plasma hyperglycemia (≥400 mg/dL) and elevated urine volume (>60 mL/d). Rat body weight and blood glucose levels were monitored weekly. Subtherapeutic levels of insulin (0–2 U neutral protamine Hagedorn [NPH] insulin administered subcutaneously daily) were administered to maintain a level of hyperglycemia of 400 to 550 mg/dL for the duration of each study. Only rats with this history of hyperglycemia were studied. Glycated hemoglobin (GHb) levels were determined by affinity chromatography, as previously described.[12]

MRI. On the day of the examination, urethane-anesthetized animals had their tail veins cannulated with a 25-gauge catheter. The dose of contrast agent (Gd-DTPA, Magnevist; Berlex Laboratories, Wayne, NJ) was 0.1 mmol/L per kilogram body weight. Each rat was then gently positioned on an MRI-compatible homemade holder with its nose placed in a plastic nose cone. Animals were allowed to breathe spontaneously during the experiment. To maintain the core temperature, a recirculating heated water blanket was used. Rectal temperature was continuously monitored while the animal was inside the magnet, as previously described.[6]

MRI data were acquired on a 4.7 T system using a two-turn transmit/receive surface coil (1-cm diameter) placed over the eye. First, high-resolution images were collected using an adiabatic spin-echo imaging sequence (repetition time [TR], 1 second; echo time [TE], 13.6 ms; number of acquisitions [NA], 4; matrix size, 512 × 512; slice thickness, 1 mm; field of view, 12 × 12 mm^2; 35 minutes/image). This resulted in an in-plane resolution of 23.4 μm^2. High-resolution images were acquired before and 2 hours after saline or distilled water provocation. After the last high-resolution image, coil tuning and matching were checked and corrected when necessary. To enhance our ability to detect subtle degrees of neuronal loss in the NMDA experiments, we acquired high-resolution images 24 hours after intraperitoneal injection of 44 mg/kg manganese chloride to better define the border between the retina and the vitreous or sclera as well as the intraretinal layers.

Images for measuring retinal ΔPo_2 and BRB integrity were then acquired, as previously described, using an adiabatic spin-echo imaging sequence (TR, 1 second; TE, 13.6 ms; NA, 1; matrix size, 128 × 256; slice thickness, 1 mm; field of view, 32 × 32 mm^2; 2 minutes/image).[6,13] This resulted in an in-plane resolution of 250 × 125 μm^2. Briefly, retinal ΔPo_2 data were collected as three images while the animal breathed room air and one image during the inhalation of carbogen. Carbogen inhalation was started at the end of the third image.[14] After returning the rat to room air for 5 minutes, dynamic contrast–enhanced (DCE) MRI was performed by collecting 12 sequential 2-minute images—three control images before the injection of contrast agent and nine images during and after a 6-second Gd-DTPA bolus injection.

Animals were removed from the magnet, and a second 2-minute inhalation challenge was performed outside the magnet, with care taken to not alter the spatial relationship between the animal head and the nose cone. At exactly 2 minutes, arterial blood from the descending abdominal aorta was collected, as described previously.[2] This blood was analyzed for glucose, PaO_2, $PaCO_2$, and pH. Note that this second inhalation challenge (outside the magnet) was needed because it was not feasible to routinely obtain an arterial blood sample from inside the magnet (>40 cm away from the magnet opening) from rats. In all cases, after blood collection, animals were euthanized with injections of intracardiac potassium chloride.

Data Analysis. To be included in this study, the animal must have demonstrated minimal eye movement during the MRI examination, nongasping respiratory pattern before and after the MRI examination, constant rectal temperatures, and positive enhancement in the anterior chamber during carbogen breathing and after Gd-DTPA injection. Based on our previous experience in rats, $n \geq 3$ is sufficient to draw statistical conclusions for BRB comparisons, and $n \geq 5$ is required to detect differences for ΔPo_2 comparisons.

Retinal Thickness. First, to ensure that we measured thickness radially (ie, perpendicularly) from the sclera (which presents as a dark line on the image), a round region-of-interest (ROI) encompassing the entire globe was drawn and its center-of-mass was determined. Radial lines were then drawn between the center-of-mass point and the edge of the round ROI associated with the retina/choroid region. Note that the high-resolution images collected for this study had sufficient spatial resolution but inadequate contrast to distinguish between retinal and choroidal circulation; combined retinal/choroidal thicknesses are reported. However, in most animals there was sufficient contrast to distinguish between distinct layers. Although the anatomic identity of all the layers is not yet known, the innermost layer appears to represent the combined width of the retinal ganglion cell, inner plexiform, and inner nuclear layers in control rats. The outer retina (combined thickness of the outer nuclear and photoreceptor layers) is less well defined with these acquisition parameters. Unfortunately, the inner-layer thickness could only be measured in two of the diabetic rats (data not shown); hence, no conclusions about possible inner retinal thickness changes were drawn from this limited data set. Inner-layer thickness was measured in regions within 1 mm of the optic nerve head. The distance between the anterior and posterior edges of the retina/choroid complex (ie, total thickness) was measured as a function of distance from the optic nerve. In this study we did not standardize the number of thickness and distance measurements obtained in each rat. To compensate, averages in 1-mm steps from the optic nerve were used for comparisons and are listed as such. For example, data sampled from 0 to 1 mm from the optic nerve are listed as 0.5 mm from the optic nerve.

MRI-Derived IOP. Initial studies indicated that minor axis length, but not major axis length, was correlated with changes in IOP (data not shown). We found that conversion of the circumference of the globe, obtained by dividing by π to produce a "derived diameter," correlated best with IOP. This derived diameter (dd) also had the advantage of being eye shape independent. In separate experiments using two untreated, different rat species (Lewis and Sprague–Dawley) or Sprague–Dawley rats infused intravenously with 20% mannitol (to lower IOP), we found, over a physiologic range of IOPs, a linear relationship between dd and applanation tonometer (Tono-Pen XL; Medtronic)–derived IOP: dd = 5.67 mm + [0.031 mm/mm Hg × IOP] ($n = 17$; $r = 0.73$; $P = 0.001$) (data not shown). Based on the slope of the calibration curve (31 μm/mm Hg), it appeared that the 23.4 μm^2 resolution of the images collected in this study (Fig. 1) should be sensitive to IOP changes ≥ 2 mm Hg. In support of this, we note that MRI-derived IOP values and applanation tonometer (Tono-Pen XL;

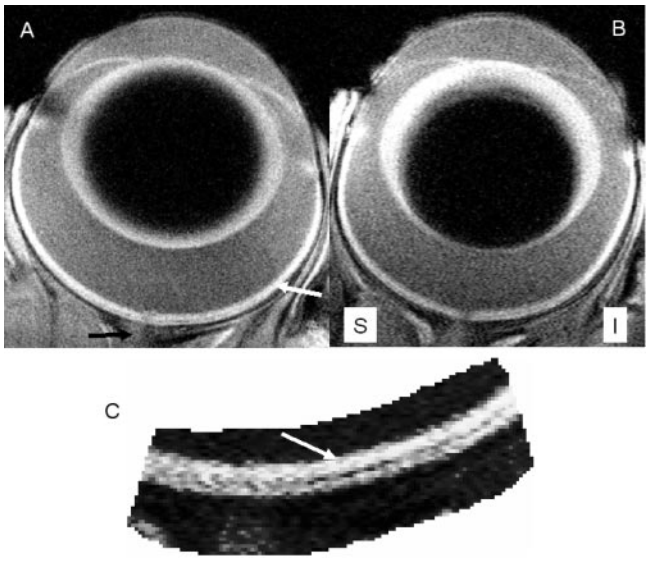

FIGURE 1. Representative high-resolution images of control (**A**) and diabetic (**B**) rat eyes (23.4 μm^2 in-plane resolution). As illustrated in (**A**), the white line in the posterior region of the eye (*white arrow*) represents the retina/choroid complex; the *black arrow* points to the optic nerve. A partial cataract is present in the diabetic rat. Superior (S) and inferior (I) are also indicated. Retinal thinning is apparent by visually comparing superior retina near the optic nerve in the diabetic rat with similar regions in the control rat. Note inferior retina regions appear similar in both (**A**) and (**B**). Quantitative confirmation of these descriptive conclusions is presented in Figure 4. (**C**) Three distinct retinal layers in the pattern light, dark, light are illustrated in a representative region of interest of a control rat. Although the anatomic identity of the middle and outer layers is not yet known, the inner layer (*white arrow*) appears to represent the combined width of the retinal ganglion cell, inner plexiform, and inner nuclear layers in control rats.

Medtronic) pressures were in agreement both 2 hours after distilled water treatment and with literature findings on lack of IOP change in diabetic rats.

ΔPo_2 and BRB Integrity. For the functional and dynamic studies, we first corrected for movement within the slice plane using an affine transformation on the images from each animal with software written in-house. Affine transformation applies a linear combination of translation, rotation, scaling, or shearing (ie, nonuniform scaling in some directions), operations that preserve lines and parallelism to coregister images to a reference image. Because the slice thickness (1 mm) is relatively large compared with the diameter of the eye (approximately 6 mm), partial volumes will be similar if the eye subtly moves out of the imaging plane, in which case the data analysis is not expected to be substantially affected. For completeness, coregistration within each experiment (ΔPo_2 and BRB) was performed on all rats used in the final analysis. After coregistration, the MRI data were transferred to a computer (Power Mac G4; Apple, Cupertino, CA) and were analyzed using the program IMAGE (a freeware program available at http://rsb.info.nih.gov/nih-image/) as detailed previously in several publications.[2,6,13,15,16]

Statistical Analysis. Data for IOP, thickness, BRB integrity, and physiologic parameters (ie, blood gas values and rectal temperatures) were consistent with a normal distribution and are presented as mean ± SEM. In most cases, comparisons between groups were performed using ANOVA, with $P < 0.05$ considered statistically significant. To examine the effect of distilled water injection on ocular physiology, a 2-tailed unpaired *t*-test was performed. Comparison of retinal ΔPo_2 between control and experimental groups was performed using a generalized estimating equation approach.[17] This method performs general linear regression analysis using all the pixels from each subject and accounts for the with-in subject correlation between adjacent pixels. In all cases, 2-tailed $P \leq 0.05$ was considered significant.

RESULTS

Systemic Physiology

Summaries of systemic physiology for the control, saline, distilled water, and diabetic groups are presented in Table 1. Few significant differences ($P < 0.05$) were observed between the groups, and all values were within the range expected for hyperoxic provocation in control animals to robustly produce measurable changes in ΔPo_2.[18] In the control, saline-, and distilled water–injected rats, GHb was not measured but plasma glucose levels were evaluated before the MRI experiment (range, 115–129 mg/dL) and fell within the expected range of values for nonfasted nondiabetic rats.[19] As expected, GHb values were significantly ($P < 0.05$) greater in the diabetic rats than in controls.

Ocular Physiology

Distilled Water Injection. IOP was not significantly different ($P > 0.05$) between noninjected control values (17.4 ± 2.1 mm Hg; $n = 9$) and at 2 hours after distilled water injection (17.2 ± 2.2 mm Hg; $n = 5$). Furthermore, no significant differences ($P > 0.05$) were found between MRI-derived IOPs of noninjected control rats (18.6 ± 4.1 mm Hg; $n = 5$), saline-treated rats (16.8 ± 3.3 mm Hg; $n = 8$), and rats 2 hours after distilled water injection (15.9 ± 1.1 mm Hg; $n = 11$).

Diabetes. MRI-derived IOPs were not different ($P > 0.05$) between control and 3-month-old diabetic rats (18.6 ± 4.1 mm Hg [$n = 5$] and 17.9 ± 1.7 mm Hg [$n = 6$], respectively).

MRI. High-resolution MRI provides a detailed and noninvasive view of ocular anatomy in vivo, including the retina/choroid complex (seen as a white line in the posterior region of the eye) and optic nerve, even in the presence of diabetes-induced cataract (Fig. 1).

TABLE 1. Summary of Model and Physiology

	Carbogen Challenge				
Group	**GHb (%)**	**P_aO_2 (mm Hg)**	**P_aCO_2 (mm Hg)**	**pH**	**Core temperature (°C)**
Control ($n = 7$)	4.0 ± 0.1	573 ± 23	51 ± 2	7.32 ± 0.01	36.3 ± 0.2
Saline ($n = 4$)	—	548 ± 6	60 ± 1	7.20 ± 0.01	36.2 ± 0.1
Distilled water ($n = 5$)	—	533 ± 21	55 ± 2	7.27 ± 0.02†	35.6 ± 0.4
Diabetes ($n = 8$)	11.9 ± 0.6*	484 ± 29*	55 ± 1	7.31 ± 0.01	36.8 ± 0.2

Values are mean ± SEM.
* $P < 0.05$, compared with control group.
† $P < 0.05$ compared with saline group.

Retinal Thickness. Thickness of inferior and superior retinas of control, saline, distilled water, and diabetic groups are presented in Figures 2 to 4. Between the control and saline groups, no significant differences ($P > 0.05$) in thickness were noted at any location panretinally. In the distilled water group, retinal/choroidal thickness was significantly ($P < 0.05$) elevated panretinally compared with the control and saline groups. In 3-month-old diabetic rats, normal retinal/choroidal thickness ($P > 0.05$) was found at most distances from the optic nerve, but retinal/choroidal thickness was subnormal ($P < 0.05$) in superior retina (0.5 mm from the optic nerve; Figs. 1 and 4).

Inner layer thickness (Fig. 1C, arrow) was significantly ($P < 0.05$) decreased in NMDA-treated eyes (63.8 ± 2.0 μm; $n = 6$) compared with control (105.4 ± 3.4 μm; $n = 4$) values. Inner thickness in the distilled water group (128.6 ± 7.4 μm; $n = 5$) was elevated ($P < 0.05$) compared with the saline (101.7 ± 1.5 μm; $n = 3$) and control groups. No significant difference ($P > 0.05$) in thickness was found between control and saline groups.

BRB Integrity. As summarized in Figure 5, no coherent increases in E values were detected in any group, implying that the BRB was intact. Note that non-zero E values occurred because of noise generated by slight motion artifacts. This noise was approximately the same across groups and did not represent a coherent buildup of contrast agent from BRB damage (data not shown). Previously, we reported a coherent buildup of contrast agent in the vitreous of 8-month-old diabetic rats relative to controls.[13]

ΔPo_2. No significant differences ($P > 0.05$) between the control and saline groups in inferior or superior hemiretinal ΔPo_2 were observed (Fig. 6). In the distilled water group, panretinal ΔPo_2 was significantly ($P < 0.05$) subnormal compared with the control and saline groups (Fig. 6). In age-matched control and 3-month-old diabetic rats, as expected, subnormal ($P < 0.05$) superior but normal ($P > 0.05$) inferior hemiretinal ΔPo_2 values were found (Fig. 7).

Discussion

In this study, we developed a model for acutely increasing retinal thickness that was associated with subnormal retinal ΔPo_2 and intact BRB. The latter two characteristics mirror those found in 3-month-old diabetic rats.[13,14] However, instead of the hypothesized increased thickness in 3-month-old diabetic rats, localized retinal thinning was found. An apparent spatial disconnect was also observed in the diabetic rats, with ΔPo_2 values subnormal pansuperiorly but retinal thinning only present in superior retina near the optic nerve. We do not have an explanation for the "local thinning" or for why changes occurred only in the superior retinas of 3-month-old diabetic rats. The rodent superior hemiretina is reported to contain a greater number of ganglion cells than the inferior hemiretina and, hence, would be expected to have a relatively greater metabolic demand.[20] We speculate that this greater metabolic demand may make the superior hemiretina more susceptible to hyperglycemic insult than the inferior hemiretina. It is also

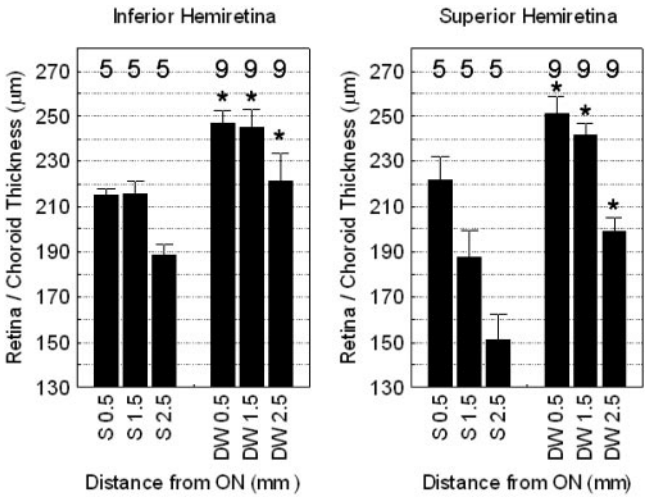

Figure 3. Plots of average inferior (*left*) and superior (*right*) retinal/choroidal thickness in saline (S) and distilled water (DW)–injected rats as a function of distance from the optic nerve (ON). Significant differences in thickness ($*P < 0.05$) were found at all locations from the ON. Numbers of animals used to generate these data are listed above each bar. Error bars represent the SEM.

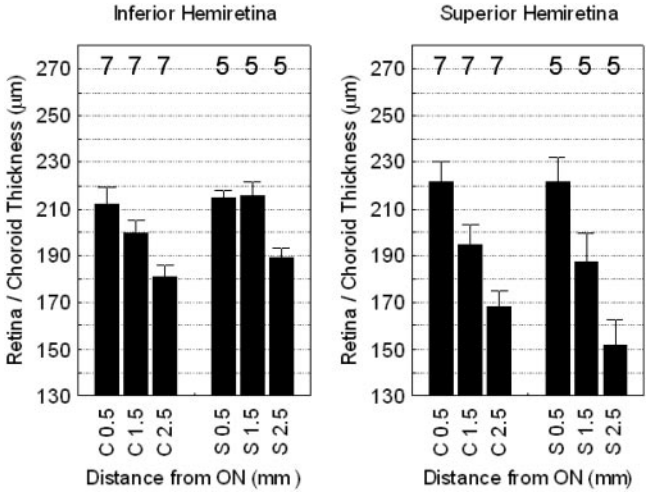

Figure 2. Plots of average inferior (*left*) and superior (*right*) retinal/choroidal thickness in control rats (C) and saline-injected (S) rats as a function of distance from the optic nerve (ON). No significant difference ($P > 0.05$) in thickness was found at any location. Numbers of animals used to generate these data are listed above each bar. Error bars represent the SEM.

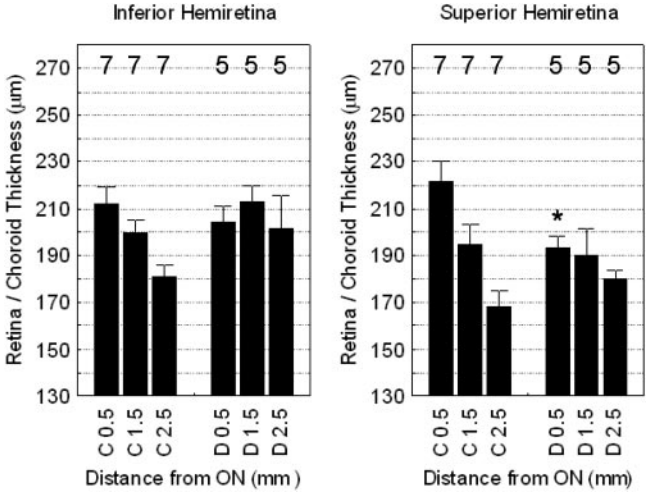

Figure 4. Plots of average inferior (*left*) and superior (*right*) retinal/choroidal thickness in control (C) and 3-month-old diabetic (D) injected rats as a function of distance from the optic nerve (ON). Numbers of animals used to generate these data are listed above each bar. Error bars represent the SEM. Significant differences in thickness ($*P < 0.05$) were found only at 0.5 mm from the ON on superior retina.

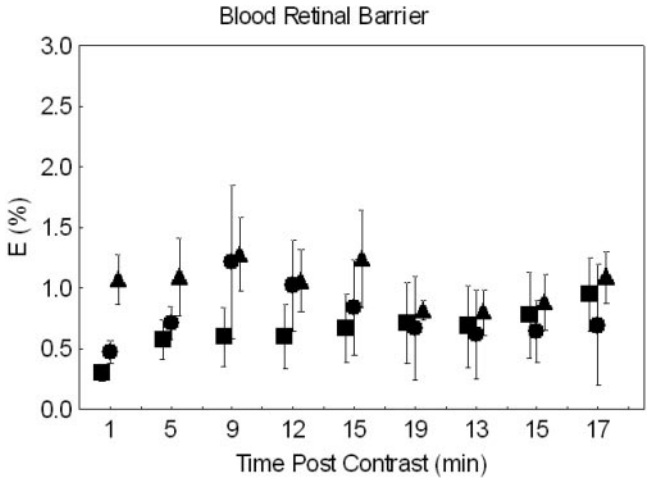

FIGURE 5. Summary of Gd-DTPA–induced signal intensity enhancement (E, %) from precontrast ($t = 0$) levels for control (■, $n = 4$), saline-injected (●, $n = 4$), and distilled water–injected (▲, $n = 4$) rats. Data are slightly shifted to aid viewing. Error bars represent the SEM. Non-zero E values occur because of noise generated by slight motion artifacts and are approximately the same across groups. Importantly, no coherent increase in E was found in any group, implying intact BRB.

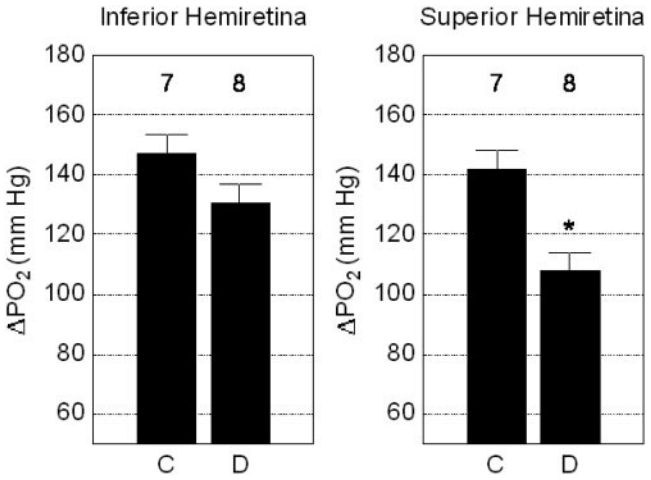

FIGURE 7. Plots of average inferior (*left*) and superior (*right*) hemiretinal ΔPo_2 during carbogen breathing in control (C) and 3-month-old diabetic (D) rats. As expected, only superior hemiretinal ΔPo_2 values of the 3-month-old diabetic rats were statistically subnormal ($^*P < 0.05$). Numbers of animals used to generate these data are listed above each bar. Error bars represent the SEM.

possible that an early diabetes-induced perturbation of metabolic-vascular coupling causes, independently, subnormal ΔPo_2 development and retinal thinning. In addition, the oxygenation response changes may occur earlier in the course of diabetes than neuronal changes or may be more sensitive to perturbed metabolic-vascular coupling. More experiments are clearly needed to further define the relationship between ΔPo_2 and neuronal activity.

Ocular Physiology

Elevated or depressed IOP may alter the regulation of ocular hemodynamics and possibly change ΔPo_2. Because distilled water–treated rats are reported to have a 22% elevated mean arterial blood pressure 2 hours after injection, it is possible that IOP was also elevated at this time.[21] In this study, at 2 hours after distilled water injection, neither direct (applanation tonometer [Tono-Pen SL; Medtronic]) nor indirect (MRI) measures of IOP revealed any differences from controls. Note that at this time, agreement was found ($P > 0.05$) between MRI-derived IOP values and applanation tonometer (Tono-Pen XL; Medtronic) pressures and that this provides additional support for the use of the calibration procedure. Taken together, changes in intraocular pressure/blood pressure do not seem to account for the roughly 64% decrease in retinal ΔPo_2 measured in distilled water–treated rats (Fig. 6).

We also found that the MRI-derived IOP in the diabetic rat group was not significantly different from that of control rats. In support of this, note that 2-month-old diabetic rats also did not demonstrate IOP different from that of controls.[22] Taken together, these considerations do not support a role for IOP in either the distilled water–treated or the diabetic rats in this study.

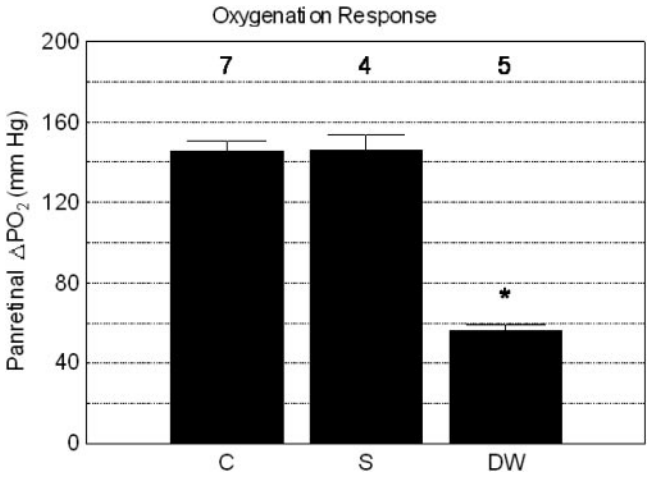

FIGURE 6. Summary of average panretinal ΔPo_2 during carbogen breathing in control (C), saline-injected (S), and distilled water–injected (DW) rats. No superior/inferior hemiretinal asymmetries were detected (data not shown); hence, only panretinal values are presented. Numbers of animals used to generate these data are listed above each bar. Error bars represent the SEM. Only the distilled water group was significantly decreased ($^*P < 0.05$) relative to the control and saline groups.

MRI Measures

Ocular Dimensions. The high-resolution MRI approach used in this study has several advantages over traditional morphometric approaches. First, it is noninvasive and so does not require enucleation and multiple-step fixation processes, which can introduce errors. Second, noninvasive measures of ocular dimensions using high-resolution A-scan ultrasonography appears to be untenable in the rat.[23] Third, retinal thicknesses are not restricted to limited retinal regions (typical about the optic nerve) but can be measured from any location from ora serrata to ora serrata, so the potential for sampling errors is reduced. Fourth, other ocular dimensions are simultaneously available from each high-resolution image, together with accurate measures of BRB integrity and ΔPo_2 from the same eye in the rat and likely in the mouse.[4,5,24,25] Diffusion-weighted images (DWIs) are used in brain studies as an index of edema and may be of value in future studies of retinal edema.[26] However, in the present study, DWI was not attempted because of the significantly smaller volume of rat retinal tissue compared with brain tissue. A limitation of the MRI method is that data are collected from a relatively thick slice (1 mm) relative to ocular diameter (approximately 6 mm in the rat), and the resultant partial volume spatial averaging

could decrease sensitivity to changes in ocular dimensions. This is not a fundamental restriction because we have collected preliminary data (not shown) that demonstrate high-quality images with a slice thickness of 0.6 mm and without increased data acquisition times (by cutting TR to 500 ms and increasing NA to 8). Another limitation is that current acquisition parameters do not provide good contrast between the choroid and the retina without contrast agent administration (data not shown). Additional studies are under way to optimize contrast between retinal layers and choroid.

The accuracy of MRI retinal morphometry was examined in three ways. First, in control rats, the maximum MRI-derived retinal thickness measured near the optic nerve (220.7 ± 22.2 μm; mean ± SD) fell within the range of published values obtained from similar locations in rats of different strains, ages, and fixation procedures (214–267 μm; adjusted assuming a choroidal thickness of 30 μm,[27,28] and Steinle J, personal communication, 2005) and could be reproducibly measured with a SD similar to our spatial resolution (23.4 μm^2 in-plane).[29–34] Choroidal thickness was not measured histologically in this study. The literature is unclear as to whether, and to what extent, choroidal thickness changes occur with diabetes.[35,36] For example, Cao et al.[36] found evidence for diabetes-related choroidal degeneration, with the percentage of focal degeneration of choroidal vessels approximately 5% to 6%.The impact of changes of this order of magnitude on choroidal thickness was not clear, especially because they reported *increased* basal laminar deposit thickness of up to 8 μm. Nagaoka et al.[35] found decreases in choroidal blood flow in the foveal region but did not measure choroidal thickness. In this case, it is unknown whether decreases in flow were related to changes in choroidal thickness or resulted from other factors. In addition, the relevance of the clinical alterations reported by Cao et al.[36] and Nagaoka et al.[35] to the diabetic rat are unclear. Of more relevance to the present study are direct measures of choroidal thickness in control and diabetic rodents.[37,38] In these studies, no changes in choroidal thickness are reported. Taken together, these considerations support the present measurements as valid for comparison of retinal thickness between control and diabetic rodents.[37,38] Second, MRI inner-layer thickness in control rats was 105.4 ± 3.4 μm, which is similar to that in the literature for the combined width of the retinal ganglion cell, inner plexiform, and inner nuclear layers in control rats (107 ± 3 μm).[33,34] We also found agreement between the MRI-detected decrease in inner layer thickness after NMDA injection (40%) relative to control eyes and the roughly 50% decreases in inner plexiform and inner nuclear layers reported in the literature.[39] These considerations support the identification of the inner layer in Figure 1C as inner retina. The agreement between the MRI-derived ocular dimensions and the literature strongly support the use of high-resolution MRI as a spatially accurate and valid method for noninvasively and simultaneously measuring important ocular dimensions in the rat.[4,5,24]

ΔPo_2. Understanding the physiology underlying normal and abnormal oxygenation responses to carbogen provocation is an active area of research in our laboratory. We considered the impact on ΔPo_2 of several systemic variables, such as baseline arterial Pao_2 and $Paco_2$, hematocrit, and ocular perfusion pressure that could have been different in diabetic or distilled water–injected rats compared with controls. Previously, we reported baseline Pao_2 and $Paco_2$ values of control rats on urethane and have collected blood samples periodically since that report to confirm that baseline blood gas values fall within similar levels in urethane-anesthetized control and diabetic rats (Pao_2, 80–100 mm Hg; $Paco_2$, 35–45 mm Hg) (data not shown).[2] Two hours after rats were injected with distilled water, no change was reported in room air arterial blood gas values and control values.[21,40] With regard to possible hematologic differences between control and diabetic rats, Alder et al.[41] reported that control and 6-week-old diabetic rats have similar hematologic parameters (except for expected elevations of blood glucose, glycated hemoglobin, and 2,3 diphosphoglycerate in the diabetic group compared with controls), including similar P50 (the Po_2 at which the oxygen-carrying capacity of blood is 50% of maximal). In control and distilled water–injected rats, plasma osmolarity, as expected, is different but hematocrit values are not.[40]

We did not measure choroidal volume or ocular blood flow in this study and so cannot directly address whether these are altered after distilled water treatment. If choroidal oxygenation substantially contributed to the preretinal vitreous ΔPo_2, then we would expect a smooth monoexponentially decaying oxygen gradient from the choroid to the vitreous during carbogen breathing. However, this type of oxygen gradient pattern was not found using intraretinal oxygen electrodes in rats during carbogen breathing.[42] Instead Yu et al.[42] reported an intraretinal minimum with a muted inner retina oxygen level increase relative to the large increases in choroidal Po_2. To further consider a possible role of choroidal oxygen on our measures, we compared ΔPo_2 and retinal thickness in control rats. If oxygen from the choroid made a significant contribution to vitreal ΔPo_2, we would expect lower ΔPo_2 over thicker central retina and higher ΔPo_2 over thinner peripheral retina. However, as shown in Figure 8, the opposite pattern was found: higher ΔPo_2 over thicker central retina and lower ΔPo_2 over thinner peripheral retina. This pattern is not consistent with the notion that the choroid makes a substantial contribution of oxygen to vitreal ΔPo_2 during carbogen breathing, at least in rats. These considerations raise the possibility that subnormal ΔPo_2 measured after distilled water injection is caused primarily by retinovascular changes.

These considerations suggest that baseline arterial Pao_2 and $Paco_2$, hematocrit, choroidal volume, and IOP values between control, diabetic, and distilled water–injected rats are unlikely to have contributed to the group differences reported in this and previous studies.[4–7] These considerations suggest that subnormal superior hemiretinal ΔPo_2 is likely caused by local physiologic retinal differences between control and experimental rats.

BRB Integrity. DCE MRI using Gd-DTPA is an established and sensitive method for monitoring BRB integrity in rabbit,

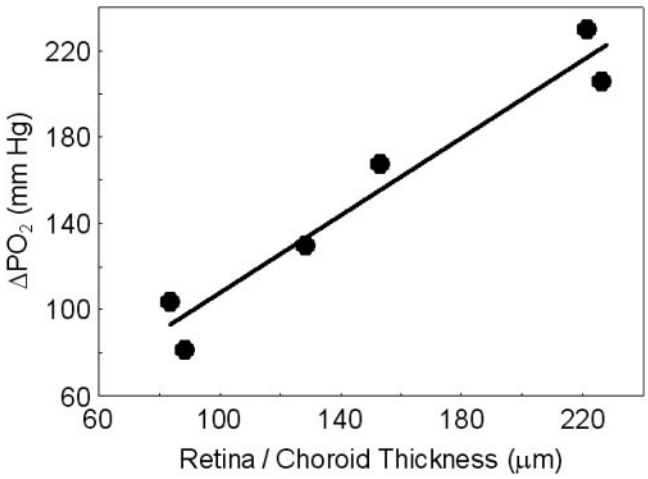

FIGURE 8. Plot of average superior and inferior ΔPo_2 compared with retinal/choroidal thickness in control rats. Each data point represents either ΔPo_2 or thickness averaged in 0- to 1-mm bins from the optic nerve. Linear regression analysis indicated a significant correlation ($P < 0.05$; $r = .97$) between these two parameters.

rat, and human.[13,16,43–52] Typically, contrast agent that passes through damaged BRB and collects in the vitreous will produce a coherent increase, or enhancement (E), of signal intensity over time relative to precontrast levels. When this happens, E can be converted to an accurate measure of BRB permeability surface area product (PS).[15,16,48,53] In this study, no coherent buildup of contrast agent was detected in the vitreous (Fig. 5). BRB PS was thus not calculated, and only E was reported.

Distilled Water Model of Intracellular Edema. Chronic intracellular fluid accumulation is thought to contribute to clinical cystoid macular edema, though a role for intracellular edema in diabetic retinopathy remains poorly investigated.[54] One reason is that a reliable model for generating intracellular retinal edema has not been available. Water intoxication is a common model of producing cerebral intracellular edema but has not yet been applied for use in the retina.[10] After injection of 15% of the rat's body weight in distilled water intraperitoneally, plasma osmolarity is lowered, producing an osmotic imbalance between blood and tissue and subsequent entry of fluid and edema. We note that it has been established that after distilled water injection, the BBB remains intact.[9,21,55–57] In this study, we found that retinal/choroidal thickness increased after distilled water injection, without evidence for BRB damage. However, specific gravity was not measured in the present study and so the presence of edema was not directly confirmed. However, increased retinal/choroidal thickness after distilled water injection is consistent with the presence of intracellular swelling/edema. The acute distilled water model is expected to be useful in future studies designed to understand the pathogenic impact and treatment of intracellular fluid accumulation in the retina.

Retinal Physiology of Diabetic Rats. We next pursued the possibility that subnormal ΔPo_2 found in 3-month-old rats with experimental diabetic retinopathy could be linked to increased retinal/choroidal thickness caused by cellular swelling.

ΔPo_2. From the present data and results in our previous reports, 3-month-old diabetic rats show subnormal superior, but not inferior, hemiretinal ΔPo_2 (Fig. 7).[4–7] Finding this asymmetry is unlikely to be the result of insufficient statistical power because inferior/superior hemiretinal response differences have been consistently found in rats and mice with experimental diabetes.[4–7]

Blood-Retina Barrier. Diabetes-induced opening of the BRB is often used as indirect evidence of an increased risk for extracellular (or vasogenic) edema formation.[58] We, and others, find no evidence for passive BRB leakage in rats until after 6 months of diabetes.[13,59–63] In sharp contrast, other laboratories report that BRB is disrupted across the entire retina as early as 2 weeks after diabetes induced in rats and measured ex vivo.[64–68] One explanation for this controversy is that ex vivo assessment of BRB damage can be confounded by death-related opening of the BRB that is unrelated to diabetes.[13] An alternative possibility is that in vivo and ex vivo methods measure different aspects of BRB integrity. The MRI approach only measures tracer levels in the vitreous, whereas ex vivo approaches only monitor tracer concentrations intraretinally. Previously, we demonstrated that DCE MRI is a sensitive approach to assaying BRB damage under a variety of conditions, including after intravitreal vascular endothelial growth factor injection.[13]

In any event, we reasoned that if previous studies are correct and BRB damage occurred as early as after 2 weeks of hyperglycemia, the 3-month point might have been enough time for edema to develop. The lack of evidence of edema in the present study is not consistent with the reported BRB damage reported by previous studies. Instead, the present thickness data support findings of an intact BRB in experimental diabetic retinopathy at 3 months. These data raise the possibility that retinal edema does not form in experimental diabetic retinopathy. To firmly address this issue, more work is needed during later durations of diabetes to determine whether retinal thickness changes.

Retinal/Choroidal Thickness. In this study, instead of increased retinal/choroidal thickness in diabetic rats, as might be expected if edema were present, significant ($P < 0.05$) retinal/choroidal thinning was observed near the optic nerve. Based on the single-slice MRI data presented in Figure 1, we were unable to determine the area of retinal thinning in terms of clock hours. Other laboratories have also reported a decrease in retinal/choroidal thickness compared with controls in regions near the optic nerve in excised rat retina after 1 month of diabetes.[37,69] The degree of retinal thinning appears to remain relatively constant (10%–15%) over time after the induction of diabetes.[37,69] The present MRI data are important because they were collected in vivo, without enucleation and fixation artifacts potentially confounding the measurements. It is possible that highly localized regions of edema are present that are below the detection sensitivity of the MRI method. This appears to be unlikely because it would be inconsistent with the apparent presence of panretinal BRB damage measured by other investigators.[64] Further, the physiologic impact of such small areas of edema would be unclear. The 3-month point was chosen because we consistently find subnormal ΔPo_2 at this time and because other investigators have found retinal thinning at longer durations of diabetes that may confound identification of retinal edema.[37] It is possible that retinal edema formation may only occur at earlier time points after the induction of diabetes. For example, Park et al.[69] claimed to have detected a transient increase in inner nuclear layer thickness at 1 week after inducing diabetes in rats. However, no statistical analysis of the data was presented to confirm that retinal/choroidal thickness actually increased over control values.[69] If edema was present in the Park et al.[69] study, it was transient and the relevance to more chronic edema typically found clinically is unclear. In any event, the apparent lack of retinal edema in 3-month-old diabetic rats in vivo implies that intracellular swelling is unlikely to underlie subnormal ΔPo_2 in diabetes. In addition, for the first time, retinal thinning is reported to be localized to superior retina near the optic nerve. We note that in 3-month-old diabetic rats, the superior retina is also the region demonstrating subnormal ΔPo_2. However, unlike retinal thinning, which appears to occur near the optic nerve, subnormal ΔPo_2 occurs across the entire superior hemiretina.[2,4–7] Efforts are now under way to better determine whether superior retinal neuronal dysfunction/loss and subnormal ΔPo_2 are linked.

Acknowledgments

The authors thank Gary Trick, Tim Kern, and James E. Olson for helpful discussions.

References

1. Berkowitz BA, McDonald C, Ito Y, Tofts PS, Latif Z, Gross J. Measuring the human retinal oxygenation response to a hyperoxic challenge using MRI: eliminating blinking artifacts and demonstrating proof of concept. *Magn Reson Med*. 2001;46:412–416.
2. Berkowitz BA. Adult and newborn rat inner retinal oxygenation during carbogen and 100% oxygen breathing: comparison using magnetic resonance imaging delta Po2 mapping. *Invest Ophthalmol Vis Sci*. 1996;37:2089–2098.
3. Berkowitz BA, Wilson CA. Quantitative mapping of ocular oxygenation using magnetic resonance imaging. *Magn Reson Med*. 1995; 33:579–581.

4. Berkowitz BA, Luan H, Gupta RR, et al. Regulation of the early subnormal retinal oxygenation response in experimental diabetes by inducible nitric oxide synthase. *Diabetes*. 2004;53:173–178.
5. Luan H, Leitges M, Gupta RR, et al. Effect of PKCbeta on retinal oxygenation response in experimental diabetes. *Invest Ophthalmol Vis Sci*. 2004;45:937–942.
6. Berkowitz BA, Ito Y, Kern TS, McDonald C, Hawkins R. Correction of early subnormal superior hemiretinal deltaPO(2) predicts therapeutic efficacy in experimental diabetic retinopathy. *Invest Ophthalmol Vis Sci*. 2001;42:2964–2969.
7. Berkowitz BA, Kowluru RA, Frank RN, Kern TS, Hohman TC, Prakash M. Subnormal retinal oxygenation response precedes diabetic-like retinopathy. *Invest Ophthalmol Vis Sci*. 1999;40:2100–2105.
8. Ferris FL III, Patz A. Macular edema: a complication of diabetic retinopathy. *Surv Ophthalmol*. 1984;28(suppl):452–461.
9. Hossmann KA. The pathophysiology of experimental brain edema. *Neurosurg Rev*. 1989;12:263–280.
10. Olson JE, Mishler L, Dimlich RV. Brain water content, brain blood volume, blood chemistry, and pathology in a model of cerebral edema. *Ann Emerg Med*. 1990;19:1113–1121.
11. Moore CG, Epley D, Milne ST, Morrison JC. Long-term non-invasive measurement of intraocular pressure in the rat eye. *Curr Eye Res*. 1995;14:711–717.
12. Kowluru RA, Tang J, Kern TS. Abnormalities of retinal metabolism in diabetes and experimental galactosemia, VII: effect of long-term administration of antioxidants on the development of retinopathy. *Diabetes*. 2001;50:1938–1942.
13. Berkowitz BA, Roberts R, Luan H, Peysakhov J, Mao X, Thomas KA. Dynamic contrast-enhanced MRI measurements of passive permeability through blood retinal barrier in diabetic rats. *Invest Ophthalmol Vis Sci*. 2004;45:2391–2398.
14. Trick GL, Berkowitz BA. Retinal oxygenation response and retinopathy. *Prog Retin Eye Res*. 2005;24:259–274.
15. Tofts PS, Berkowitz BA. Rapid measurement of capillary permeability using the early part of the dynamic Gd-DTPA MRI enhancement curve. *J Magn Reson*. 1993;102(series B):129–136.
16. Berkowitz BA, Tofts PS, Sen HA, Ando N, de Juan E Jr. Accurate and precise measurement of blood-retinal barrier breakdown using dynamic Gd-DTPA MRI. *Invest Ophthalmol Vis Sci*. 1992;33:3500–3506.
17. Liang Z. Longitudinal data analysis using generalized linear models. *Biometrika*. 1986;73:13–22.
18. Berkowitz BA. Role of dissolved plasma oxygen in hyperoxia-induced contrast. *Magn Reson Imaging*. 1997;15:123–126.
19. Vallon V, Huang DY, Deng A, Richter K, Blantz RC, Thomson S. Salt-sensitivity of proximal reabsorption alters macula densa salt and explains the paradoxical effect of dietary salt on glomerular filtration rate in diabetes mellitus. *J Am Soc Nephrol*. 2002;13:1865–1871.
20. Dreher B, Potts RA, Ni YK, Bennett MR. The development of heterogeneities in distribution and soma sizes of rat retinal ganglion cells. In: Stone J, Dreher B, Rapaport DH, eds. *Development of Visual Pathways in Mammals.* New York: Alan R. Liss; 1984:39–57.
21. Olson JE, Banks M, Dimlich RV, Evers J. Blood-brain barrier water permeability and brain osmolyte content during edema development. *Acad Emerg Med*. 1997;4:662–673.
22. Kanamori A, Nakamura M, Mukuno H, Maeda H, Negi A. Diabetes has an additive effect on neural apoptosis in rat retina with chronically elevated intraocular pressure. *Curr Eye Res*. 2004;28:47–54.
23. Guggenheim JA, Creer RC, Qin XJ. Postnatal refractive development in the Brown Norway rat: limitations of standard refractive and ocular component dimension measurement techniques. *Curr Eye Res*. 2004;29:369–376.
24. Roberts R, Zhang W, Ito Y, Berkowitz BA. Spatial pattern and temporal evolution of retinal oxygenation response in oxygen-induced retinopathy. *Invest Ophthalmol Vis Sci*. 2003;44:5315–5320.
25. Ito Y, Berkowitz BA. MR studies of retinal oxygenation. *Vision Res*. 2001;41:1307–1311.
26. Albensi BC, Knoblach SM, Chew BG, O'Reilly MP, Faden AI, Pekar JJ. Diffusion and high resolution MRI of traumatic brain injury in rats: time course and correlation with histology. *Exp Neurol*. 2000;162:61–72.
27. Steinle JJ, Smith PG. Sensory but not parasympathetic nerves are required for ocular vascular remodeling following chronic sympathectomy in rat. *Auton Neurosci*. 2003;109:34–41.
28. Steinle JJ, Pierce JD, Clancy RL, Smith G. Increased ocular blood vessel numbers and sizes following chronic sympathectomy in rat. *Exp Eye Res*. 2002;74:761–768.
29. Aizu Y, Oyanagi K, Hu J, Nakagawa H. Degeneration of retinal neuronal processes and pigment epithelium in the early stage of the streptozotocin-diabetic rats. *Neuropathology*. 2002;22:161–170.
30. Fukuchi T, Takahashi K, Shou K, Matsumura M. Optical coherence tomography (OCT) findings in normal retina and laser-induced choroidal neovascularization in rats. *Graefes Arch Clin Exp Ophthalmol*. 2001;239:41–46.
31. Chaudhuri A, Hallett PE, Parker JA. Aspheric curvatures, refractive indices and chromatic aberration for the rat eye. *Vis Res*. 1983;23:1351–1363.
32. Remtulla S, Hallett PE. A schematic eye for the mouse, and comparisons with the rat. *Vis Res*. 1985;25:21–31.
33. Buttery RG, Hinrichsen CF, Weller WL, Haight JR. How thick should a retina be? A comparative study of mammalian species with and without intraretinal vasculature. *Vis Res*. 1991;31:169–187.
34. Hughes WF. Quantitation of ischemic damage in the rat retina. *Exp Eye Res*. 1991;53:573–582.
35. Nagaoka T, Kitaya N, Sugawara R, et al. Alteration of choroidal circulation in the foveal region in patients with type 2 diabetes. *Br J Ophthalmol*. 2004;88:1060–1063.
36. Cao J, McLeod S, Merges CA, Lutty GA. Choriocapillaris degeneration and related pathologic changes in human diabetic eyes. *Arch Ophthalmol*. 1998;116:589–597.
37. Barber AJ, Lieth E, Khin SA, Antonetti DA, Buchanan AG, Gardner TW. Neural apoptosis in the retina during experimental and human diabetes: early onset and effect of insulin. *J Clin Invest*. 1998;102:783–791.
38. Barber AJ, Antonetti DA, Kern TS, et al. The Ins2Akita mouse as a model of early retinal complications in diabetes. *Invest Ophthalmol Vis Sci*. 2005;46:2210–2218.
39. Honjo M, Tanihara H, Kido N, Inatani M, Okazaki K, Honda Y. Expression of ciliary neurotrophic factor activated by retinal Müller cells in eyes with NMDA- and kainic acid-induced neuronal death. *Invest Ophthalmol Vis Sci*. 2000;41:552–560.
40. Stummer W, Betz AL, Shakui P, Keep RF. Blood-brain barrier taurine transport during osmotic stress and in focal cerebral ischemia. *J Cereb Blood Flow Metab*. 1995;15:852–859.
41. Alder VA, Yu DY, Su EN, Cringle SJ. Comparison of hematologic parameters in normal and streptozotocin-induced diabetic rats. *Lab Anim Sci*. 1992;42:170–173.
42. Yu DY, Cringle SJ, Alder V, Su EN. Intraretinal oxygen distribution in the rat with graded systemic hyperoxia and hypercapnia. *Invest Ophthalmol Vis Sci*. 1999;40:2082–2087.
43. Wilson CA, Fleckenstein JL, Berkowitz BA, Green ME. Preretinal neovascularization in diabetic retinopathy: a preliminary investigation using contrast-enhanced magnetic resonance imaging. *J Diabetes Complications*. 1992;6:223–229.
44. Funatsu H, Wilson CA, Berkowitz BA, Sonkin PL. A comparative study of the effects of argon and diode laser photocoagulation on retinal oxygenation. *Graefes Arch Clin Exp Ophthalmol*. 1997;235:168–175.
45. Metrikin DC, Wilson CA, Berkowitz BA, Lam MK, Wood GK, Peshock RM. Measurement of blood-retinal barrier breakdown in endotoxin-induced endophthalmitis. *Invest Ophthalmol Vis Sci*. 1995;36:1361–1370.
46. Wilson CA, Berkowitz BA, Funatsu H, et al. Blood-retinal barrier breakdown following experimental retinal ischemia and reperfusion. *Exp Eye Res*. 1995;61:547–557.
47. Ando N, Sen HA, Berkowitz BA, Wilson CA, de Juan E Jr. Localization and quantitation of blood-retinal barrier breakdown in experimental proliferative vitreoretinopathy. *Arch Ophthalmol*. 1994;112:117–122.
48. Berkowitz BA, Wilson CA, Tofts PS, Peshock RM. Effect of vitreous fluidity on the measurement of blood-retinal barrier

permeability using contrast-enhanced MRI. *Magn Reson Med*. 1994;31:61–66.

49. Sato Y, Berkowitz BA, Wilson CA, de Juan E Jr. Blood-retinal barrier breakdown caused by diode vs argon laser endophotocoagulation. *Arch Ophthalmol*. 1992;110:277–281.
50. Sen HA, Berkowitz BA, Ando N, de Juan E Jr. In vivo imaging of breakdown of the inner and outer blood-retinal barriers. *Invest Ophthalmol Vis Sci*. 1992;33:3507–3512.
51. Wilson CA, Berkowitz BA, Sato Y, Ando N, Handa JT, de Juan E Jr. Treatment with intravitreal steroid reduces blood-retinal barrier breakdown due to retinal photocoagulation. *Arch Ophthalmol*. 1992;110:1155–1159.
52. Berkowitz BA, Sato Y, Wilson CA, de Juan E. Blood-retinal barrier breakdown investigated by real-time magnetic resonance imaging after gadolinium-diethylenetriaminepentaacetic acid injection. *Invest Ophthalmol Vis Sci*. 1991;32:2854–2860.
53. Tofts PS, Berkowitz BA. Measurement of capillary permeability from the Gd enhancement curve: a comparison of bolus and constant infusion injection methods. *Magn Reson Imaging*. 1994; 12:81–91.
54. Bringmann A, Reichenbach A, Wiedemann P. Pathomechanisms of cystoid macular edema. *Ophthalmic Res*. 2004;36:241–249.
55. Olson JE, Katz-Stein A, Reo NV, Jolesz FA. Evaluation of acute brain edema using quantitative magnetic resonance imaging: effects of pretreatment with dexamethasone. *Magn Reson Med*. 1992;24: 64–74.
56. Yamaguchi M, Wu S, Ehara K, Nagashima T, Tamaki N. Cerebral blood flow of rats with water-intoxicated brain edema. *Acta Neurochir Suppl (Wien)*. 1994;60:190–192.
57. Olson JE, Evers JA, Banks M. Brain osmolyte content and blood-brain barrier water permeability surface area product in osmotic edema. *Acta Neurochir Suppl (Wien)*. 1994;60:571–573.
58. Lund-Andersen H. Mechanisms for monitoring changes in retinal status following therapeutic intervention in diabetic retinopathy. *Surv Ophthalmol*. 2002;47(suppl 2):S270–S277.
59. Ennis SR. Permeability of the blood-ocular barrier to mannitol and PAH during experimental diabetes. *Curr Eye Res*. 1990;9:827–838.
60. Ennis SR, Betz AL. Sucrose permeability of the blood-retinal and blood-brain barriers: effects of diabetes, hypertonicity, and iodate. *Invest Ophthalmol Vis Sci*. 1986;27:1095–1102.
61. Lightman S, Pinter G, Yuen L, Bradbury M. Permeability changes at blood-retinal barrier in diabetes and effect of aldose reductase inhibition. *Am J Physiol*. 1990;259:R601–R605.
62. Caspers-Velu LE, Wadhwani KC, Rapoport SI, Kador PF. Permeability of the blood-retinal and blood-aqueous barriers in galactose-fed rats. *J Ocul Pharmacol Ther*. 1995;11:469–487.
63. Lightman S, Rechthand E, Terubayashi H, Palestine A, Rapoport S, Kador P. Permeability changes in blood-retinal barrier of galactosemic rats are prevented by aldose reductase inhibitors. *Diabetes*. 1987;36:1271–1275.
64. Xu Q, Qaum T, Adamis AP. Sensitive blood-retinal barrier breakdown quantitation using Evans blue. *Invest Ophthalmol Vis Sci*. 2001;42:789–794.
65. Vinores SA, McGehee R, Lee A, Gadegbeku C, Campochiaro PA. Ultrastructural localization of blood-retinal barrier breakdown in diabetic and galactosemic rats. *J Histochem Cytochem*. 1990;38: 1341–1352.
66. Enea NA, Hollis TM, Kern JA, Gardner TW. Histamine H1 receptors mediate increased blood-retinal barrier permeability in experimental diabetes. *Arch Ophthalmol*. 1989;107:270–274.
67. Murata T, Ishibashi T, Khalil A, Hata Y, Yoshikawa H, Inomata H. Vascular endothelial growth factor plays a role in hyperpermeability of diabetic retinal vessels. *Ophthalmic Res*. 1995;27:48–52.
68. Jones CW, Cunha-Vaz JG, Rusin MM. Vitreous fluorophotometry in the alloxan- and streptozocin-treated rat. *Arch Ophthalmol*. 1982; 100:1141–1145.
69. Park SH, Park JW, Park SJ, et al. Apoptotic death of photoreceptors in the streptozotocin-induced diabetic rat retina. *Diabetologia*. 2003;46:1260–1268.